

Condition Monitoring of Induction Motors Using Hilbert and Fourier Transforms

Elsa ALLARD¹, Kishore Bingi^{2,*}, P. Arun Mozhi Devan², Nurul Fauzana Imran Gulcharan², Rosdiazli Ibrahim², Madiah Omar³

¹Department of Electronics, Polytech Dijon, Dijon, France

²Department of Electrical and Electronics Engineering, Universiti Teknologi PETRONAS, Seri Iskandar, Malaysia

³Department of Integrated Engineering, Universiti Teknologi PETRONAS, Seri Iskandar, Malaysia

*Email: bingi.kishore@utp.edu.my

Abstract—Ensuring the reliable operation of induction motors is crucial in industrial environments, where unexpected failures can result in costly downtime and safety risks. This study presents a signal-based approach for condition monitoring of induction motors operating under real industrial conditions. A total of 10 motors from a refinery plant were analysed using two key signal processing techniques: the Hilbert Transform for envelope and instantaneous frequency analysis in the time domain, and the Fast Fourier Transform (FFT) for spectral analysis in the frequency domain. Motor current signals were acquired from a central control station, enabling non-invasive diagnostics. Fault-sensitive features were extracted from both domains and normalised to compute a composite health score, which serves as an indicator of motor condition. The analysis revealed that Hilbert-based temporal features are susceptible to early fault symptoms, while FFT-based spectral features provide robustness in identifying fault types and severity. The proposed methodology supports the implementation of condition-based maintenance strategies, enhancing reliability and operational efficiency in industrial environments.

Keywords—Condition monitoring, Fast Fourier transform, Hilbert transform, Induction motor, Signal processing

I. INTRODUCTION

Induction motors, the most widely used machine, are employed in a broad range of applications, including pumps, power plants, wind turbines, conveyors, compressors, and various automated systems [1], [2]. However, like any rotating machinery, induction motors are susceptible to various failures that can impact their performance and longevity. The most predominant failures of these motors include bearing faults, stator winding issues, rotor bar defects, and air gap eccentricities [3]. Among these, bearing faults are widespread, accounting for a substantial portion of induction motor failures. Bearing degradation typically arises from lubrication problems, contamination, fatigue, or improper installation, leading to increased vibration, heat generation, and, ultimately, motor failure if not detected promptly [4], [5].

Recently, several advanced techniques have been proposed to detect bearing faults in induction motors at an early stage. For instance, the use of machine learning algorithms combined with vibration signal analysis has been employed to classify different bearing fault types in various motor configurations [6]. Other studies have explored methods such as Motor Current Signature Analysis, acoustic emission monitoring,

thermal imaging, and advanced signal processing techniques, including the wavelet transform and Hilbert Transform, aiming to improve detection sensitivity and diagnostic accuracy. These approaches are particularly valuable because they offer non-invasive solutions, allowing continuous monitoring of motor health without interrupting the regular operation [7].

In [7], a method for diagnosing induction motors using MCSA combined with the Hilbert transform was proposed. The study shows a 30-60% improvement in characteristic fault amplitudes and reliable detection of various internal faults. In [8], the researchers combine the Hilbert transform with wavelet analysis, coupled with a neuro-fuzzy system, to diagnose motor conditions from vibration signals. The approach shows significant robustness to speed variations and reliable classification between healthy and faulty states. A statistical approach based on the Weibull distribution and applied to vibration signals processed by the Hilbert transform [9]. This method enables early detection of bearing faults, even when they are invisible to the naked eye.

Dias et al. presented a technique that combines the Hilbert transform with an adaptive filtering algorithm of the normalised least mean squares type [10]. This approach enables the simultaneous detection of multiple faults, such as defective bearings or broken bars, while maintaining stable performance even in noisy industrial environments. In [11], the authors exploit the Hilbert transform to extract the envelope of current signals and then use an artificial neural network to classify faults. This method achieves a classification rate of over 95%, even under low-load conditions. In [12] and [13], a comparison of three signal processing methods is carried out, namely, the Fourier transform (FFT), the short-time Fourier transform (STFT), and the wavelet transform (WT). The study highlights the limitations of the FFT for non-stationary signals, while the STFT offers better time-frequency resolution. WT, meanwhile, stands out for its early detection capabilities.

To complement these detection techniques, RUL prediction has emerged as an essential tool for condition monitoring. Estimating RUL involves predicting the time remaining before a motor or one of its components fails based on historical data and real-time measurements. By training models on characteristics extracted from vibration signals, it becomes possible to monitor the degradation of critical components,

such as bearings, over time [14]. The integration of RUL predictions enables maintenance teams to plan interventions optimally, reduce unplanned stoppages and extend motor life.

Motivated by the above literature, this research aimed to apply advanced signal processing methods to a set of 10 induction motors from the refinery plant to assess their state of health, compare the respective performances of the Hilbert and FFT transforms, and estimate the health score. The study also aims to identify reliable indicators of bearing degradation that can support the implementation of condition-based maintenance strategies. The remaining part of the article is organised as follows: Section II outlines the methodology employed, highlighting the primary techniques used, including Hilbert transform, FFT, and health score methods. Section III presents and discusses the results obtained through the various techniques. Section IV offers key observations.

II. METHODOLOGY

The methodology flowchart employed in this study is shown in Fig. 1. As shown in the figure, the methodology involves acquiring motor signals, preprocessing them, and applying Hilbert and Fourier Transforms to extract fault-sensitive features. These features are normalised and combined to compute a health score, which classifies motors as Healthy, Degraded, or Faulty. Results guide maintenance decisions for improved reliability and performance.

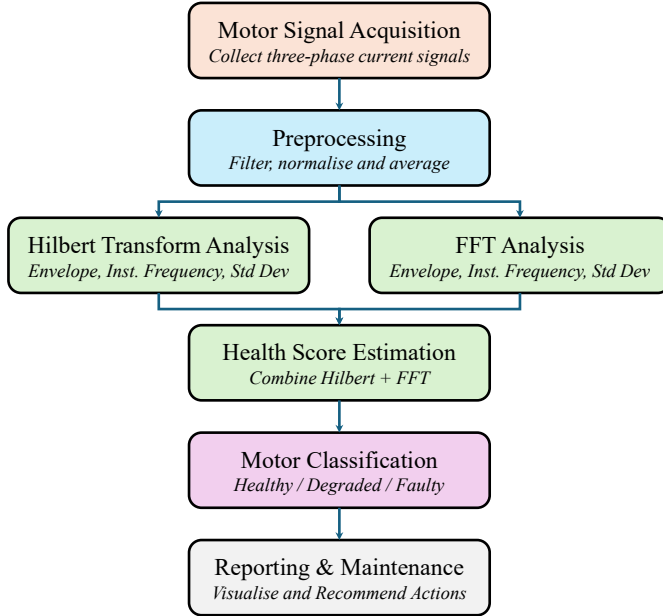


Fig. 1. Methodology flowchart for condition monitoring of induction motors using Hilbert and Fourier Transforms.

A. Hilbert Transform

The Hilbert transform is a mathematical operation that transforms a real signal into a complex analytical signal. This analytical signal consists of a fundamental component and an imaginary component. Combining these two parts calculates

the signal's envelope, a measure of its instantaneous amplitude. Mathematically, if $x(t)$ is the input signal, its Hilbert transform $\hat{x}(t)$ is defined by:

$$\hat{x}(t) = \frac{1}{\pi} P \int_{-\infty}^{\infty} \frac{x(\tau)}{t - \tau} d\tau, \quad (1)$$

where P denotes the Cauchy principal value.

The analytical signal, envelope and instantaneous frequency are given respectively as follows,

$$z(t) = x(t) + j\hat{x}(t), \quad |z(t)| = \sqrt{x^2(t) + \hat{x}^2(t)}, \quad (2)$$

$$f(t) = \frac{1}{2\pi} \times \frac{d}{dt} [\arg(z(t))]. \quad (3)$$

Then, the standard deviation of this instantaneous frequency is used as a health indicator, which is calculated as follows:

$$\sigma_f = \sqrt{\frac{1}{N} \sum_{i=1}^N (f_i - \mu)^2}, \quad (4)$$

where

- f_i is the instantaneous frequency at time index i ,
- N is the total number of samples and
- μ is the mean of the instantaneous frequencies, computed as $\mu = \frac{1}{N} \sum_{i=1}^N f_i$.

B. Fast Fourier Transform (FFT)

The FFT algorithm converts a signal from the time domain to the frequency domain. The aim is to represent a complex signal $x(t)$ as the sum of sinusoids of different frequencies. This makes it possible to visualise which frequency components are present in the signal and their corresponding amplitudes. Mathematically, for a discrete signal $x[n]$, the discrete Fourier transform is given by:

$$X[k] = \sum_{n=0}^{N-1} x[n] \cdot e^{-j2\pi kn/N}, \quad (5)$$

where

- N is the total number of samples,
- $X[k]$ is the frequency component at index k .

Given measured maximum and minimum values, the averaged signal for each phase is:

$$x_{\text{avg}}(t) = \frac{x_{\max}(t) + x_{\min}(t)}{2}. \quad (6)$$

The magnitude at each frequency is computed as follows:

$$M(f_k) = |X(f_k)| = \sqrt{\Re(X(f_k))^2 + \Im(X(f_k))^2}. \quad (7)$$

The mean magnitude of overall positive frequencies is:

$$\overline{M} = \frac{1}{N'} \sum_{k=1}^{N'} M(f_k), \quad (8)$$

where N' is the number of positive frequency bits.

The phase is considered healthy if $\overline{M} < \text{Threshold}$, else it is diagnosed as unhealthy. FFT is initially used to identify the characteristic frequencies associated with bearing faults.

TABLE I
SUMMARY OF HEALTH INDICATORS AND CLASSIFICATION RESULTS FOR INDUCTION MOTORS BASED ON HILBERT AND FFT ANALYSIS

Motor ID	Hilbert			FFT		Health Score Estimation	
	Average Frequency (Hz)	Standard Deviation	State	Average Magnitude	State	Health Score	State
E22802-05	0.0254	0.000972	Healthy	77.83	Healthy	0.90	Healthy
E22802-06	0.0256	0.001306	Healthy	80.66	Healthy	0.85	Healthy
E22802-08	0.0253	0.000992	Healthy	91.81	Healthy	0.94	Healthy
E22807-01	0.0255	0.000895	Healthy	80.42	Healthy	0.88	Healthy
E22807-02	0.0254	0.000781	Healthy	81.74	Healthy	0.89	Healthy
E22812-01	0.0271	0.007830	Faulty	29500	Healthy	0.55	Degraded
E22812-02	0.0269	0.006950	Degraded	30000	Healthy	0.48	Degraded
E22902-01	0.0262	0.005320	Degraded	45000	Healthy	0.75	Healthy
E22902-02	0.0261	0.005080	Degraded	48000	Healthy	0.72	Healthy
E22902-04	0.0264	0.006110	Degraded	47000	Healthy	0.71	Healthy

Then, we can visualise the distribution of signal energy in the frequency domain, allowing us to track the evolution of fault-related harmonics over time. In this way, one can effectively assess the mechanical condition of motors based on the signals.

C. Health Score Estimation

The overall health score (H_s) of an induction motor is computed by combining the normalised FFT magnitude and the normalised standard deviation of instantaneous frequency derived from the Hilbert transform, as expressed by the following equation:

$$H_s = 1 - ((0.5 \times \text{SHI}) + (0.5 \times \text{THI})) \quad (9)$$

where SHI is the Spectral Health Indicator, which reflects the normalised magnitude from FFT analysis, and THI is the temporal health indicator, which represents the normalised standard deviation of instantaneous frequency from the Hilbert transform.

High values of the indicators denote normal behaviour. A lower score indicates a worse state of health. Depending on the score obtained, each motor is classified in one of three categories:

- Healthy: $H_s > 0.7$
- Degraded: $0.4 < H_s \leq 0.7$
- Faulty: $H_s \leq 0.4$

III. RESULTS AND DISCUSSION

This section presents the performance analysis of all compared motors using Hilbert and FFT transforms to estimate the H_s of the motors. Table I shows the overall numerical and statistical analysis of all the considered 10 motors. Further, the signal envelopes and frequency spectra derived from the Hilbert transforms and FFT analysis for all compared motors are shown in Figs. 2 and 3, respectively.

A. Hilbert Transform

From Fig. 2 and Table I, it can be seen that for motor E22802-05, analysis of the signal envelopes derived from the Hilbert transforms across the three phases, A, B, and C, indicates a stable and balanced performance. The envelopes

consistently range from 52 to 58, with phase B showing slightly higher amplitudes. The instantaneous frequencies fluctuate between 0.026 and 0.028 Hz with minimal variation. Thus, indicating no anomalies are detected, resulting in a favourable health assessment (Healthy). Similarly, the motor E22802-06 exhibits oscillations within the range of 44-50, displaying regular variations typical of normal operation. Phase B exhibits slightly elevated amplitudes, while phase A displays edge effects. Instantaneous frequencies remain stable between 0.025 and 0.028 Hz. The motor exhibits excellent mechanical stability and is assessed as Healthy. Further, the envelopes of motor E22802-08 range from 57 to 65 with good coherence across phases. Phase B shows slight dominance, but all phases are well-aligned. Frequencies are consistent between 0.025 and 0.027 Hz. No faults are detected, and the motor is classified as Healthy. The envelopes fluctuate between 54 and 62 with regular oscillations for motor E22807-01. Phase B shows slightly higher values, but the pattern remains stable. Frequencies range from 0.025 to 0.027 Hz with minor dispersion. The motor operates under balanced conditions and is deemed Healthy. For motor E22807-02, the envelopes oscillate between 58 and 65, with phase B consistently showing higher amplitudes. Despite this asymmetry, the motor remains stable. Frequencies are uniform between 0.025 and 0.028 Hz. No critical faults are observed, and the motor is considered Healthy.

On the other hand, the envelopes of motor E22812-01 show agitation, especially in phases A and B, with amplitudes ranging from 30 to 35. Irregularities and frequency fluctuations around 0.027 Hz suggest instability. The motor exhibits moderate disturbance and is diagnosed as Faulty. Moreover, for motor E22812-02, the envelopes are more regular (29-34) than the previous motor, with closely spaced phases and a slightly elevated B phase. Frequencies hover around 0.026 Hz with moderate dispersion. The motor shows early signs of fatigue and is classified as Degraded. Similarly, the envelopes of motor E22902-01 reach up to 54 with consistent phase spacing. Frequencies centre around 0.026 Hz, indicating reliable performance. However, the standard deviation approaches the critical threshold, suggesting the motor is Degraded and requires monitoring. Also, the envelopes of motor E22902-



Fig. 2. Signal envelopes derived from the Hilbert transforms for all compared motors.

02 oscillate between 40 and 48 with intense phase alignment. Frequencies are coherent around 0.025 Hz, and dispersion is minimal. Although classified as degraded, the motor performs effectively and is close to the Healthy threshold. For the final motor E22902-04, the envelopes fluctuate between 42 and 48 with slight agitation toward the end. Phase B shows elevated readings, and initial noise is present. Frequencies remain stable around 0.026 Hz. The motor is stable but exhibits performance fluctuations, warranting a Degraded classification.

B. Fast Fourier Transform

Similarly, from Fig. 3 and Table I, for motor E22802-05, the frequency spectrum across phases A, B, and C exhibits a high-magnitude peak near 0 Hz, exceeding 50,000 units, indicating a strong DC component and balanced operation. The spectrum is clean with minimal harmonics, confirming fault-free performance. Additionally, motor E22802-06 exhibits a dominant low-frequency peak at approximately 43,000-44,000 units, with consistent spectral patterns across all phases. The absence of significant harmonics and the near-perfect overlap

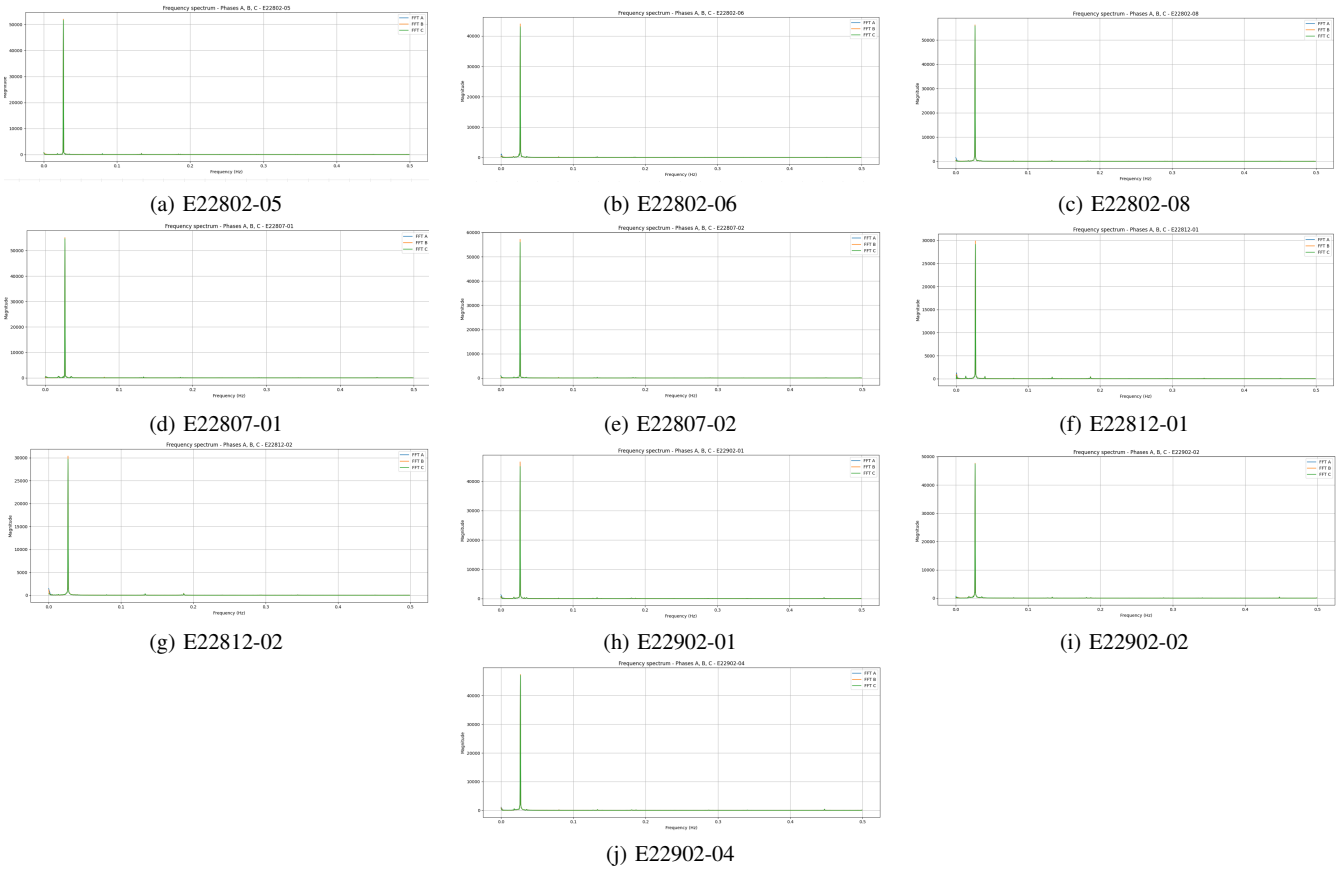


Fig. 3. Frequency spectrum derived from the FFT analysis for all compared motors.

of phase spectra affirm its stable and healthy condition.

Motor E22802-08 demonstrates exceptional phase balance, with a prominent peak of approximately 55,000 units near 0 Hz and a flat spectrum beyond this point. The minimal presence of harmonics below 0.1 Hz underscores its robust mechanical and electrical performance. Likewise, motor E22807-01 exhibits a precise and uniform FFT profile, with a peak at approximately 57,000 units and negligible high-frequency components. The spectral alignment across phases confirms a well-functioning and balanced system. Motor E22807-02 continues this trend, displaying a coherent spectral profile with a dominant peak of 58,000 units and no signs of electrical imbalance or vibration issues, indicating efficient operation.

In contrast, motor E22812-01 exhibits a lower peak magnitude of approximately 30,000 units at a frequency of around 0.025 Hz. Although the phase curves are similar, the reduced spectral energy and faint low-frequency lines suggest moderate disturbance and a degraded condition. Motor E22812-02 also exhibits a primary peak near 30,000 units with consistent phase alignment. However, the lower amplitude and absence of distortions indicate early signs of degradation.

Motor E22902-01 exhibits a distinct peak at 0.025 Hz with an amplitude of nearly 45,000 units. The closely aligned phase spectra and quiet frequency range indicate minimal harmonic interference and a healthy motor state. Motor E22902-02 exhibits a strong low-frequency peak of 48,000 units, char-

acterised by excellent phase synchronisation and a smooth spectrum, confirming optimal performance. Finally, motor E22902-04 exhibits a prominent peak of approximately 47,000 units at 0.025 Hz, with a consistent energy distribution across phases and only minor secondary peaks, indicating stable operation with no significant faults.

C. Health Scores

The graph presented in Fig. 4 provides a detailed overview of the health status of all the compared motors. This assessment is performed through sophisticated signal processing techniques that utilise both the Fourier and Hilbert Transform methodologies. The resulting data is quantified into a Health Score that ranges from 0 to 1, effectively summarising the operational integrity of each motor. This Health Score is instrumental in categorising motors into three distinct states based on their performance and reliability. A score greater than 0.7 signifies that a motor is in a “Healthy” condition, indicating optimal functionality and minimal risk of failure. A score that falls between 0.4 and 0.7 classifies a motor as “Degraded,” suggesting that although the motor is still operational, it may require attention or monitoring to prevent future issues. Finally, a score of 0.4 or lower categorises a motor as “Faulty,” highlighting urgent concerns regarding its performance and an imminent need for maintenance or replacement.

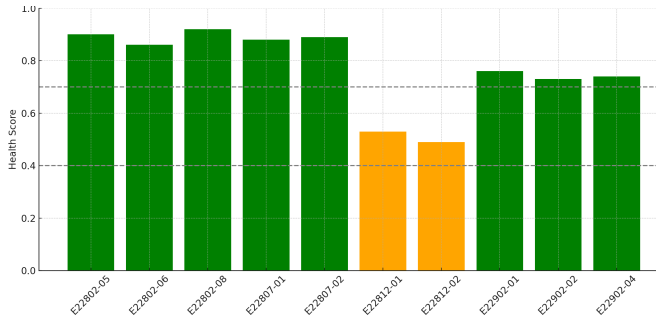


Fig. 4. Estimated health score for all compared motors.

In the predictive maintenance that relies on the H_s of motors, the score assigned to each motor can be interpreted as an indicator of its ageing process. Specifically, when motors receive a score exceeding 0.7 (for instance, within the range of E22802-08 to E22807-02), they are deemed to be operating at full capacity. This high score implies that there is no immediate need for maintenance or intervention, as these motors are functioning optimally. Conversely, motors that score between 0.4 and 0.7 (e.g., between E22812-01 and E22812-02) exhibit noticeable signs of wear and deterioration. While still functional, these motors warrant closer observation over time, as their Remaining Useful Life is expected to decrease as the score continues to decline. It is important to note that, at this point, no motor displayed in the graph has reached a critical condition. However, should any motor's score dip below 0.4, it would raise a significant concern, indicating that the motor is approaching the end of its functional lifespan. In a predictive system, crossing this threshold triggers a red alert status, indicating a minimal estimated time before failure, thereby necessitating immediate intervention or maintenance planning to prevent unexpected downtime or equipment failure.

IV. CONCLUSION

This study presents a robust signal-based framework for condition monitoring of induction motors using Hilbert and Fourier Transform techniques. The Hilbert transform is a powerful analytical tool for detecting minor variations in signals, making it effective for early fault detection in machinery. It enhances sensitivity to subtle changes, allowing timely interventions that can prevent major failures. Additionally, the FFT provides a detailed frequency spectrum of a motor, helping to identify structural issues such as rotor imbalances. By transforming time-domain signals into the frequency domain, the FFT enables engineers to visualise motor vibrations and detect anomalies that indicate mechanical problems. Also, incorporating a health scores estimator enhances assessments by translating physical indicators into predictive maintenance timelines. Experimental results from ten motors in a refinery plant validate the approach, showing consistent performance in detecting mechanical degradation. This methodology supports proactive maintenance strategies, providing a non-invasive and scalable solution for enhancing operational reliability and

minimising downtime in industrial environments. This synergistic use of the Hilbert transform, FFT, and H_s estimation offers a reliable motor health assessment, supporting proactive maintenance strategies and aligning with goals of reliability and performance improvement.

ACKNOWLEDGEMENT

Universiti Teknologi PETRONAS supported this research through the Short Term Internal Research Fund (STIRF), Grant No: 015LA0-074.

REFERENCES

- [1] U. Sengamalai, G. Anbazhagan, T. Thamizh Thentral, P. Vishnuram, T. Khurshaid, and S. Kamel, "Three phase induction motor drive: a systematic review on dynamic modeling, parameter estimation, and control schemes," *Energies*, vol. 15, no. 21, p. 8260, 2022.
- [2] N. Z. Zulkifli, B. Ramadevi, K. Bingi, R. Ibrahim, and M. Omar, "Predicting remaining useful life of induction motor bearings from motor current signatures using machine learning," *Machines*, vol. 13, no. 5, p. 400, 2025.
- [3] N. S. B. Rosli, R. B. Ibrahim, I. Ismail, and K. Bingi, "Application of principal component analysis vs. multiple linear regression in resolving influential factor subject to air booster compressor motor failure," in *2018 IEEE 4th International Symposium in Robotics and Manufacturing Automation (ROMA)*. IEEE, 2018, pp. 1–5.
- [4] F. Xu, N. Ding, N. Li, L. Liu, N. Hou, N. Xu, W. Guo, L. Tian, H. Xu, C.-M. L. Wu *et al.*, "A review of bearing failure modes, mechanisms and causes," *Engineering Failure Analysis*, vol. 152, p. 107518, 2023.
- [5] S. Muthukumaran, A. Rammohan, S. Sekar, M. Maiti, and K. Bingi, "Bearing fault detection in induction motors using line currents," *ECTI Transactions on Electrical Engineering, Electronics, and Communications*, vol. 19, no. 2, pp. 209–219, 2021.
- [6] R. M. Chagas and W. M. Santos, "Study of the application of mcsa at induction motors of a roller table," in *2024 3rd International Conference on Advancement in Electrical and Electronic Engineering (ICAEEE)*. IEEE, 2024, pp. 1–6.
- [7] A. El Idrissi, A. Derouich, S. Mahfoud, N. El Ouanjli, A. Chantoufi, A. S. Al-Sumaiti, and M. A. Mossa, "Bearing fault diagnosis for an induction motor controlled by an artificial neural network—direct torque control using the hilbert transform," *Mathematics*, vol. 10, no. 22, p. 4258, 2022.
- [8] P. Konar and P. Chattopadhyay, "Multi-class fault diagnosis of induction motor using hilbert and wavelet transform," *Applied Soft Computing*, vol. 30, pp. 341–352, 2015.
- [9] M. Abd-el Malek, A. K. Abdelsalam, and O. E. Hassan, "Induction motor broken rotor bar fault location detection through envelope analysis of start-up current using hilbert transform," *Mechanical Systems and Signal Processing*, vol. 93, pp. 332–350, 2017.
- [10] C. G. Dias and L. C. da Silva, "Induction motor speed estimation based on airgap flux measurement using hilbert transform and fast fourier transform," *IEEE Sensors Journal*, vol. 22, no. 13, pp. 12 690–12 699, 2022.
- [11] B. Saddam, A. Aissa, B. S. Ahmed, and S. Abdellatif, "Detection of rotor faults based on hilbert transform and neural network for an induction machine," in *2017 5th International Conference on Electrical Engineering-Boumerdes (ICEE-B)*. IEEE, 2017, pp. 1–6.
- [12] Y. Liu, L. Guo, Q. Wang, G. An, M. Guo, and H. Lian, "Application to induction motor faults diagnosis of the amplitude recovery method combined with FFT," *Mechanical Systems and Signal Processing*, vol. 24, no. 8, pp. 2961–2971, 2010.
- [13] N. Mehalia and R. Dahiya, "A comparative study of FFT, STFT and wavelet techniques for induction machine fault diagnostic analysis," in *Proceedings of the 7th WSEAS international conference on computational intelligence, man-machine systems and cybernetics, Cairo, Egypt*, vol. 2931, 2008.
- [14] M. A. Bermeo-Ayerbe, V. Cocquempot, C. Ocampo-Martinez, and J. Diaz-Rozo, "Remaining useful life estimation of ball-bearings based on motor current signature analysis," *Reliability Engineering & System Safety*, vol. 235, p. 109209, 2023.